Journal of Civil Structural Health Monitoring (2020) 10:627–637
https://doi.org/10.1007/s13349-020-00406-3

ORIGINAL PAPER

Distributed fiber optic sensing along driven ductile piles: Design, sensor installation and monitoring benefits

Christoph M. Monsberger[1] · **Werner Lienhart**[1] · **Martin Hayden**[2]

Received: 27 January 2020 / Revised: 24 April 2020 / Accepted: 6 May 2020 / Published online: 7 June 2020

Abstract
Efficient and economic foundations are essential to ensure the long-term integrity of structures. Driven ductile piles offer a safe and quick solution for foundations, which can be individually customized to changing soil conditions. Geotechnical load tests on a small subset of piles can be performed at large construction sites to examine the bearing capacity for optimization purposes. Arising deformations during these statical tests are usually measured using electrical sensors at the top, which, however, do not deliver information about the stress distribution along the pile. This paper presents a fiber optic monitoring approach, which provides distributed strain profiles with a spatial resolution of up to 10 mm along driven ductile piles. The high measurement resolution of about 1 $\mu m/m$ enables the detection of local effects in the load transfer from the pile to the surrounding grout and soil. The critical sensor installation on-site as well as results of various field applications with pile lengths of up to 25 m are presented. Verification measurements at the pile's head and internal measurements of strain gauges prove the suitability of the developed monitoring approach and demonstrate the high potential of distributed fiber optic sensing for applications in soil mechanics.

Keywords Distributed fiber optic sensing · Driven ductile pile · Field monitoring · Geotechnical load tests · Soil mechanics

1 Introduction

To ensure long-term integrity of constructions, an efficient and economic foundation is a critical aspect in civil engineering. On large construction sites, hundreds of piles may be installed and geotechnical load tests are usually performed on a small subset of piles to prove the bearing capacity and finally, to optimize the pile lengths. It is state of the art to measure the arising deformations during these tests at the pile head using electrical sensors, which only deliver an average displacement over the entire length. Nevertheless, the load transfer from the pile to the soil is not uniform in reality and, therefore, new sensing techniques are required to derive the stress distribution along piles.

Testing of reinforced concrete piles using distributed fiber optic sensors (DFOS) has gained more interest in recent years, see, e.g. [1, 24, 26]. DFOS systems were also successfully used for long-term monitoring of, e.g. concrete tension piles [25].

Driven ductile piles enable a safe and quick solution in foundation engineering as the pile length can be individually adjusted to changing soil conditions. However, the DFOS installation is considerably more critical compared to concrete piles as the optical sensing fiber has to survive the extremely harsh driving process. This might be the reason why DFOS monitoring concepts for driven piles only rarely exist in the literature (see, e.g. [10]). Over the last 5 years, our institute (Institute of Engineering Geodesy and Measurement Systems, IGMS) in cooperation with Keller Grundbau Ges.mbH (Austria) has developed a DFOS approach to monitor distributed strain profiles along driven ductile piles [17, 18]. For this, a tailored and reliable installation technique had to be found, which is not only able to protect

✉ Christoph M. Monsberger
christoph.monsberger@tugraz.at

Werner Lienhart
werner.lienhart@tugraz.at

Martin Hayden
martin.hayden@keller.com

[1] Institute of Engineering Geodesy and Measurement Systems, Graz University of Technology, Steyrergasse 30, 8010 Graz, Austria

[2] Keller Grundbau Ges.mbH, Guglgasse 15, 1110 Wien, Austria

the sensing fiber during the driving process but also does not adversely affect the construction process itself.

This paper reports about our 5 years' experience in ductile pile monitoring using distributed fiber optic sensors. In the following, we shortly review the setup of the DFOS system, including the sensing technology, the different strain sensing cables and the system calibration. The critical sensor installation process during the pile construction is introduced and results of various field tests in different soils are presented. Finally, the utilization of the DFOS approach for continuous monitoring of uplifts at a construction pit as well as the related outcomes are discussed and an outlook on further research aspects is given.

2 Distributed fiber optic sensing in geotechnical applications

In recent years, distributed fiber optic monitoring systems have become significantly more popular in geotechnical applications as they can provide distributed strain and temperature measurements with a high accuracy along the entire object without any gaps. In the literature, various different examples can be found, where DFOS systems were used to monitor tunnels [13, 14, 30], geotechnical structural elements [4, 20], pipelines [2, 12] or reinforced earth structures [22]. For this, however, the fiber optic interrogation unit, the sensing cable and the installation technique must be appropriately adjusted to guarantee the quality of the measurement results.

2.1 Sensing principles

The basic principle of DFOS systems (Fig. 1a) is based on natural scattering of an optical pulse during the forward propagation along the sensing fiber. Small parts of the scattered light are reflected back to the interrogation unit and can be used there for sensing purposes. As depicted in Fig. 1 (b), the backscattering spectrum can be split into linear (Rayleigh) and non-linear (Brillouin and Raman) scattering effects. In general, Raman-based systems are only sensitive to temperature, whereas Rayleigh and Brillouin instruments are sensitive to both strain and temperature changes. Their capabilities regarding spatial resolution and measurement accuracy are, however, significantly different: Rayleigh backscattering systems provide a very high spatial resolution of some millimeters with a measurement resolution of about 1 $\mu m/m$ [16], but are mostly limited to sensing ranges of about 70 m. Sensing units based on Brillouin scattering enable measurements over tens of kilometers [23], which, however, results in limitations of the spatial resolution (between 0.1 and 10 m, depending on the sensing range) and the measurement precision (about 4– 10 $\mu m/m$). Further information about the different sensing principles can be found in [7].

The field applications described in this paper cover pile lengths between 10 and 25 m, this is why a Rayleigh scattering system from Luna Innovations Inc. (OBR 4600) is used for sensing. Based on the optical frequency domain reflectometry (OFDR) technique, this instrument enables distributed strain sensing with a spatial resolution of about 10 mm and a typical measurement frequency in the range of

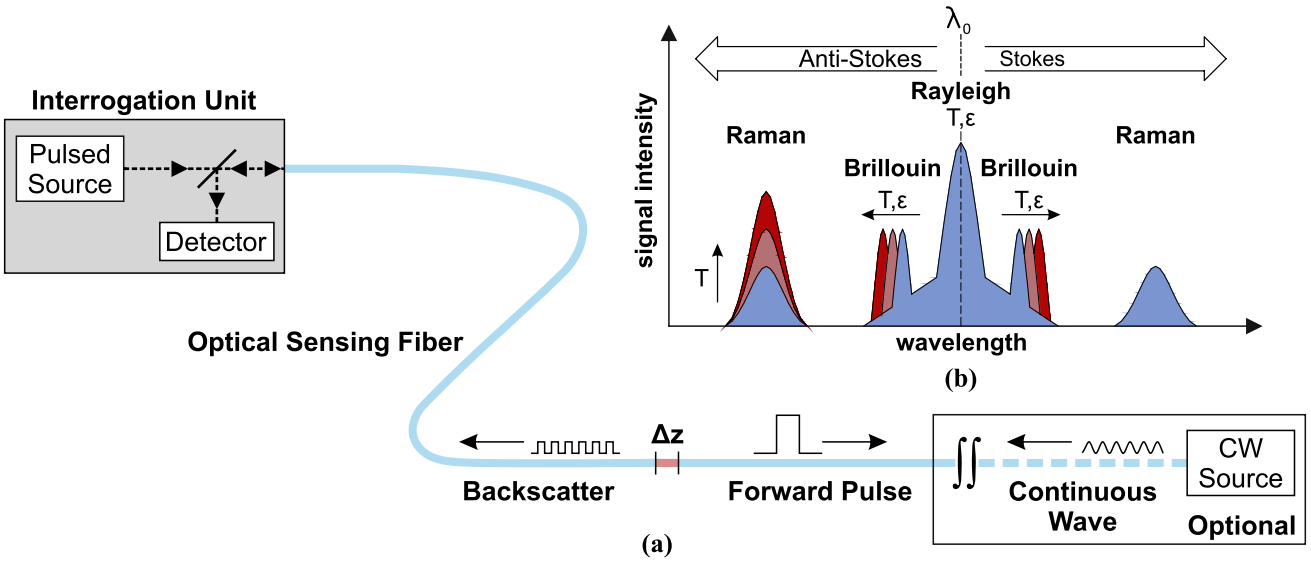

Fig. 1 Distributed fiber optic sensing techniques: **a** basic scheme of sensing setup (based on [15]) and **b** different scattering components in optical glass fibers (based on [6])

about 0.1 Hz, even in the harsh environment at a construction site. Nevertheless, the designed DFOS approach can be interrogated with any other fiber optic measurement system, including Brillouin sensing units for strain and temperature sensing or even single mode Raman instruments for temperature sensing only.

2.2 Strain sensing cables

Due to harsh environments on site, robust sensing cables are required to ensure the integrity of the sensing fiber during the driving process. For that reason, IGMS normally uses prefabricated sensing cables from Solifos AG (Switzerland) to measure strain along the piles. Figure 2 shows the setup of two cable types [27, 28], which are especially developed for sensing in concrete or grout material. The optical fiber is protected by a metal tube (types V3 and V9) or even by a special steel armoring (type V3) and, therefore, the cables show good resistance against mechanical impacts. The outer surface of both cables is structured to provide a solid connection with the surrounding grout material. Furthermore, all layers of the cables are interlocking to ensure a reliable strain transfer from the outer sheet to the sensitive glass fiber core. Monsberger et al. (2017) give further information about different strain sensing cables from Solifos AG [19].

2.3 System calibration

Analogous to conventional sensors, a sensor characteristic curve is required to derive strain values from the raw measurement quantity (e.g. wavelength, frequency or intensity of backscattered signal). Nevertheless, manufacturers of fiber optic sensing cables often do not provide their own calibration parameters and refer to literature values instead, which might result in errors of several percent, see, e.g. [22]. IGMS developed a unique calibration facility [31], which enables highly precise, fully automatic calibration of strain sensors with lengths of up to 30 m under stable laboratory conditions. Prior to field measurements, individual calibrations of several samples of the used sensing cables are usually carried out to reliably determine the frequency-to-strain relation. Results of various calibrations of different sensing cables for geotechnical applications from Solifos AG (e.g. types V3 and V9) are shown in [19].

Temperature compensation of the derived strain values basically depends on the monitoring application. Since the optical fiber is vertically embedded into the ground along the pile, the temperature should be almost constant during geotechnical load tests, in which the investigation period is relatively short (typically $<$ 24 hours). In other applications, especially in long-term monitoring, an additional sensing cable, which is not influenced by strain, must be installed nearby the strain sensor to eliminate arising temperature effects.

3 Pile construction and sensor installation

The "Keller Ductile Pile" (KDP) is an example for commonly used driven ductile piles. One single pile element usually has a length of 5 m, a diameter between 118 and 170 mm and a wall thickness between 7.5 and 13 mm. For construction, the first pile element is equipped with a driving shoe and pushed into the ground using a hydraulic quick impact hammer, see Fig. 3a. Subsequently, the next element is inserted into a conical collar (pile coupling) at the upper end of the first one. The elements become frictionally engaged due to the hydraulic hammer impacts during the further driving process. The pile can be variably extended to its final length, where it reaches a load-bearing soil layer. This layer is currently determined by measuring

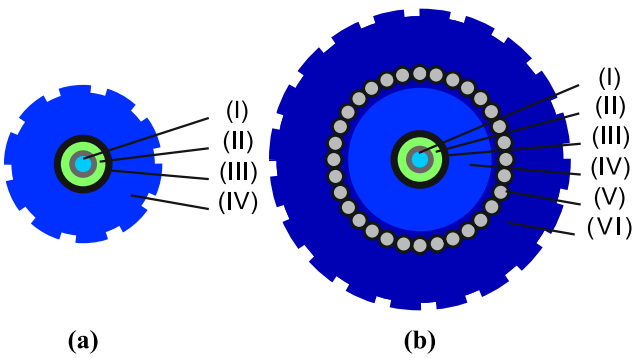

Fig. 2 Setup of different Solifos strain sensing cables [17]: **a** type V9 and **b** type V3 with (I) strain sensing single mode fiber (ø250 $\mu m/m$), (II) multi-layer buffer with strain transfer layer, (III) metal tube, (IV) polyimide protection layer, (V) special steel armoring and (VI) polyimide outer sheath

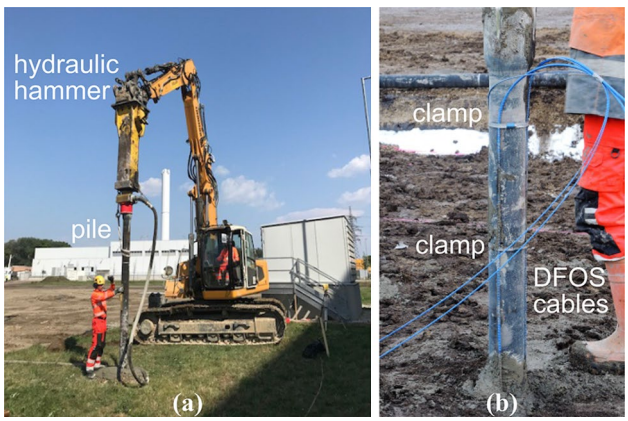

Fig. 3 DFOS-driven ductile pile [17]: **a** pile driving process; **b** installation of fiber optic sensing cables along the pile

the penetration speed during pile driving. KDPs are basically compression-grouted, which means that the driving shoe has a slightly larger diameter than the pile. While driving the pile, the shoe compresses the surrounding soil material and a cavity is formed, which is instantly filled with grout. After the grout is cured, it forms a rigid connection with the surrounding ground and contributes to the bearing capacity of the pile.

During the pile construction, the hydraulic hammer generates accelerations of up to 2000 m/s^2 and extremely harsh conditions (e.g. loose gravel) are prevalent for the optical sensing cables. Our installation experiences show that presented cable types are robust enough to withstand the environmental impacts if the cable is reliably attached to the pile and additionally protected in critical areas, e.g. at the pile couplings. Beside the critical sensor protection, the installation method must be also practical and quick in order to prevent major interference with the construction process of the pile. Laboratory tests, in which different mounting techniques were investigated, point out that attaching the cable using customary collar clamps (Fig. 3b) with a spacing between 0.5 and 1 m (depending on the pile diameter) is sufficient to ensure a fixed position of the cable during the driving process. The structured surface of the sensing cables finally forms a rigid bond with the surrounding material after the grout is hardened.

4 Static load tests and measurement results

The bearing capacity of compression-grouted piles basically depends on a combination of the shaft friction and the toe resistance. These quantities are derived in static load tests, in which either tension or compression is applied to the pile. Innovative setups also allow the separate determination of both quantities with one test only, e.g. the Pile HAY-Proof-System ® [8]. Usually, the shaft friction is not uniform along the pile and varies depending on the prevalent soil conditions in different depths. The developed DFOS sensing system enables the localization of variations in the strain distribution along the pile and, therefore, gives new insights into the load transfer from the pile to the soil.

As an example for measurement results in tension tests, so called pull-out tests, Fig. 4 depicts the strain profiles measured by the DFOS system along various ductile piles in different soils. The different, heterogeneous strain distributions demonstrate that the load transfer from the pile to the soil and, therefore, the shaft friction is related to the prevalent soil conditions.

Test results in uniform soil with fine sand and gravel (Fig. 4a) display an inhomogeneous strain distribution with almost equidistantly spaced peaks. It is assumed that these peaks can be related to cracks in the grout material [19], which arise at higher load steps due to the progressive failure

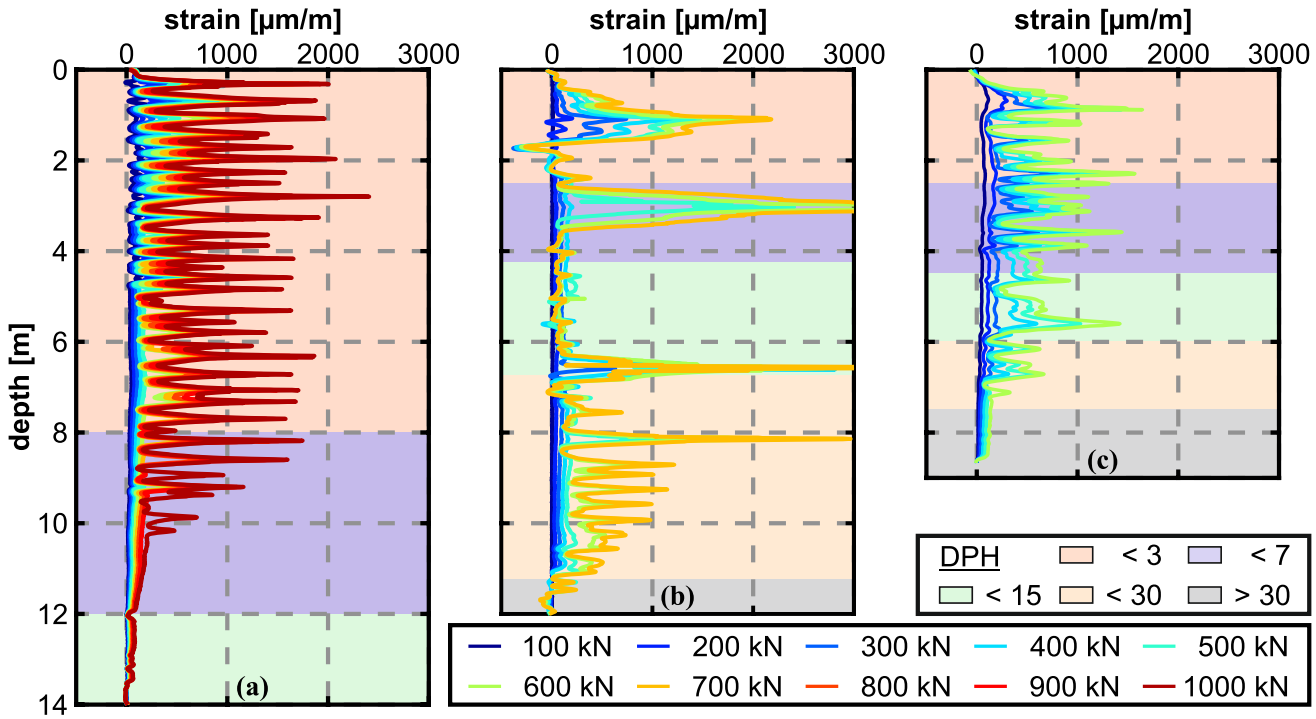

Fig. 4 Strain profiles measured by the DFOS system along various ductile piles in different soils during pull-out tests and corresponding results of dynamic probing (DPH) [17]: **a** fine sand and gravel; **b** silt and clay; **c** clay and gravels

of the grout material. No strain peaks are visible in higher depths at the highest load step. This means that the shaft friction of the pile does not fail at the maximum load of 1000 kN. The DFOS system enables an exact detection of the range of this area, which probably could lead to an optimization of the pile lengths at this construction site.

The strain values in other soils in Fig. 4 (b), (c) display a different pattern in comparison to the strain profiles in the homogeneous soil in Fig. 4 (a). Especially in the mixed soil consisting of silt and clay (Fig. 4b), sections with almost no strain (e.g. between 3.5 and 6.5 m) are followed by extremely high-strain peaks (e.g. at 6.5 m), which suggest extremely varying soil conditions and transition zones between different soil layers along the pile. This assumption can be confirmed by results of dynamic probing heavy (DPH), which was performed at each construction site nearby the instrumented pile. The corresponding results, displayed in Fig. 4 in impacts per 10 cm penetration depth, show very different bulk density variations at each test, especially significantly higher variations in inhomogeneous soils (Fig. 4b) compared to homogeneous soils (Fig. 4a).

Nevertheless, the measured strain distribution always combines the soil conditions and the material properties of the pile itself (wall thickness, grouting diameter). These stiffness parameters usually also vary along the pile depending on the in situ construction as well as the manufacturing quality of the pile elements and must be taken into account for any detailed analysis of the soil conditions.

The evolution of cracks in grout material as a result of its progressive failure is typically illustrated as strain peaks in the DFOS profiles. Figure 5 shows strain profiles along the pile's top part measured simultaneously by the DFOS system along cable type V3 (Fig. 5a) and V9 (Fig. 5b) during one selected pull-out test. Basically, both cable types depict a similar behavior and almost all of the crack positions can be identified in both figures at the same location. Nevertheless, cable type V9 seems to be more sensitive to local effects due to the less massive design of the cable (Fig. 2). This enables also a detection of smaller peaks (#01), which are not visible along the profiles of type V3. In addition, type V9 is able to separate different cracks that arise very close to each other (#02). Consequently, the shape and magnitude of the strain peak itself not only depends on the prevalent crack width, but also on the design of the used sensing cable and must be well selected to the application regarding protection and sensitivity.

To verify the DFOS results, the strain values along the pile can be numerically integrated from the bottom point to the pile head by

$$d = \sum_{i=1}^{n} (\epsilon_i \, \Delta z), \tag{1}$$

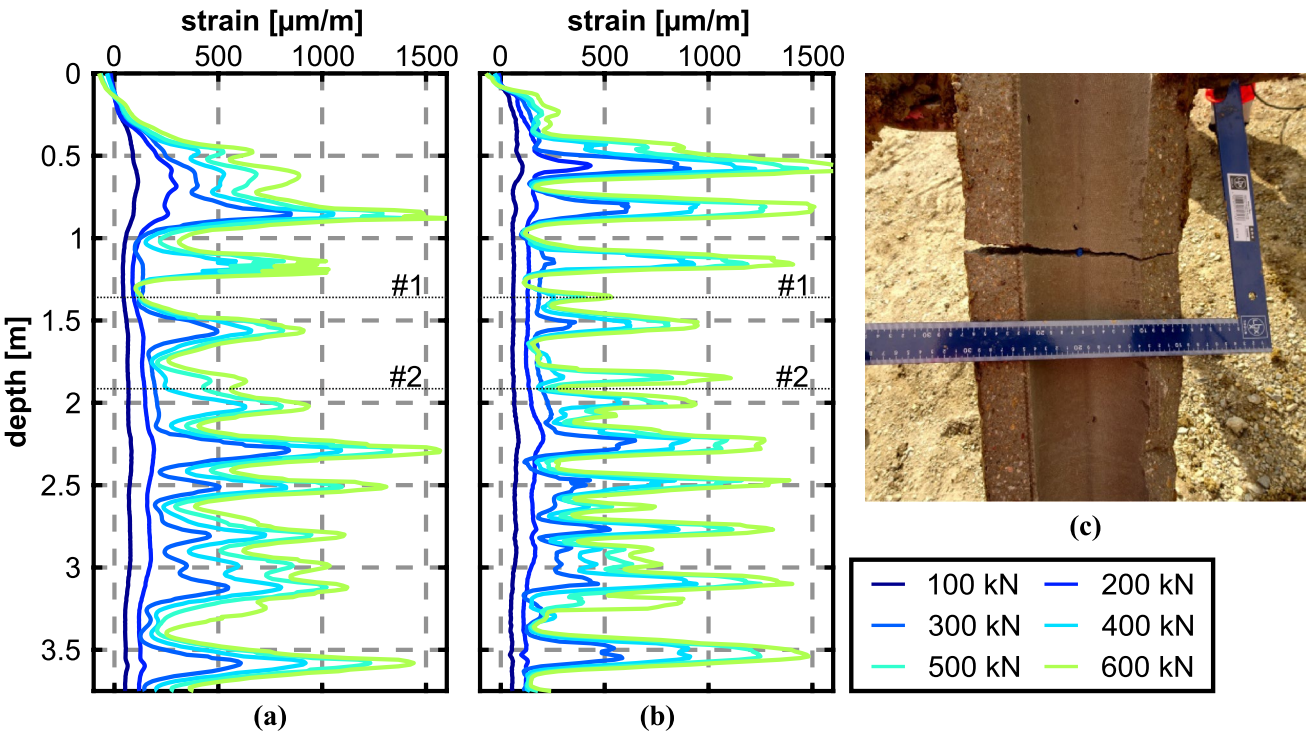

Fig. 5 Analysis of crack evolution in the grout material: **a** DFOS strain profiles along sensing cable V3; **b** DFOS strain profiles along sensing cable V9 and **c** small part of grout material excavated after the test

where ϵ is the strain value along the pile, Δz is the spatial resolution of the DFOS system and d the resulting displacement at the pile head, which can be compared to the results of conventional linear variable distance transducers (LVDT). The measuring armatures of these LVDTs are usually mounted on a stable supporting structure next to the pile (Fig. 6a), which is not affected by the loading forces, and measure the relative distance changes to glass plates mounted at the pile head. The time series of the applied loads of one selected pull-out test (strain profiles already displayed in Fig. 4a) and the load–displacement curves, separately derived from both technologies, are displayed in Fig. 6 (b), (c).

The independent sensing methods basically depict a good agreement within the first loading cycle up to 400 kN. Larger hysteresis effects are, however, visible in the LVDT data after the first loading, when the pile is released. Since the LVDTs can be confirmed by total station measurements to prism targets at the pile head (Fig. 6a), these effects are caused by an absolute movement of the pile, which, of course, cannot be captured by the DFOS system and results in a constant offset between the data sets after the release. Although the shape of the load–displacement curves of both technologies show a similar behavior, this effect further increases at higher load steps.

To provide an independent in situ measurement technique for verification purposes, strain gauges may be installed along the pile to compare the DFOS results. Such an installation along the outer sheet of the pile is, however, critical due to extreme impacts acting on the pile and, therefore, on the electrical sensors, during the construction. To ensure the integrity of the sensors, a reinforcement bar was especially prepared for one pile test and seven strain gauges were applied at different depths. The reinforcement bar was inserted in the grout material in the middle of the pile (see Fig. 7 a).

The instrumented pile was investigated within a compression test. To avoid effects related to curvature because of the non-centric position of the optical fibers, four optical sensing cables were mounted in different positions around the pile. The average strain profile of all fibers at each load step is shown in Fig. 7 (b). These profiles depict a uniform increase of the negative strain level with increasing load. Furthermore, the negative strain decreases from the pile head, where the load is applied, to the pile toe. Anomalies in the strain profiles at the pile head and at the pile coupling in a depth of about 4 m are related to, among others, an additional protection of the sensing cables at these positions. As a result of this protection, the arising strain might not be completely transferred to the sensing cables at these locations. Except for these areas, the shape of the measured values of the strain gauges in Fig. 7 (c) shows good agreement to the fiber optic measurement results. Deviations might be related to the different position of the sensors, slight inhomogeneities in the grout material or the undefined position of the rebar inside the pile and thus bending effects, which can be captured effectively only by the DFOS sensing approach due to the distributed sensing capabilities.

In addition to the evaluation of the strain distribution in longitudinal direction, the arrangement of the fiber optic sensing cables (Fig. 7a) also enables the determination of bending effects in transversal direction of the pile. In case of arising curvature along the object, two sensing fibers mounted at opposite sides (e.g. DFOS #01 and #03) must show a different strain behavior and the curvature can be derived from the strain values $\epsilon_{1/3}$ by

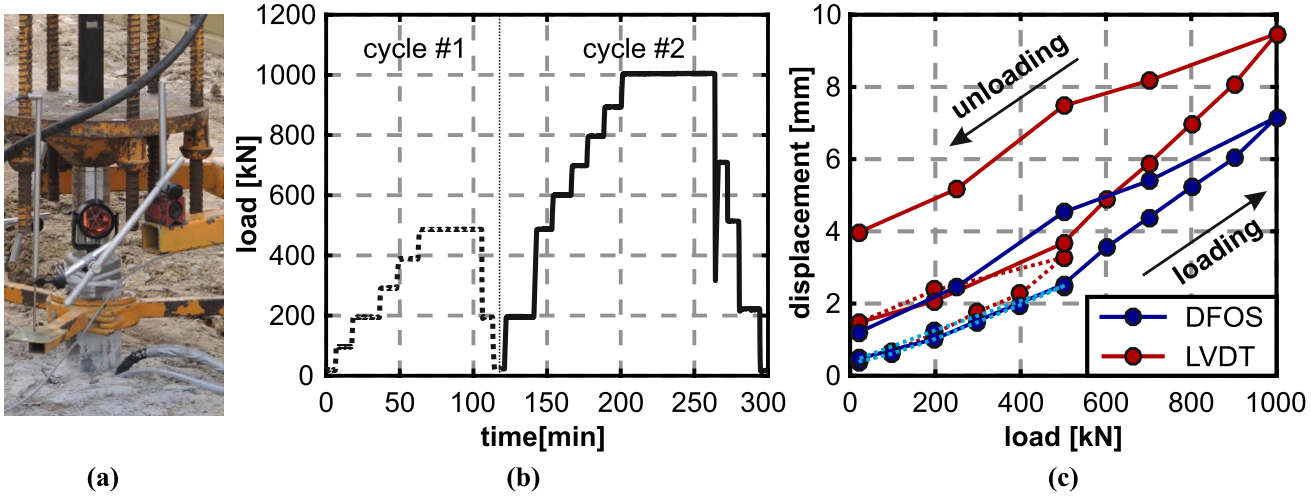

Fig. 6 Comparison between conventional sensors and fiber optic measurement system: **a** position of LVDT sensors at pile head; **b** applied loads over time during one selected test; **c** load–displacement curves calculated from LVDT measurements at the pile head and derived from DFOS system

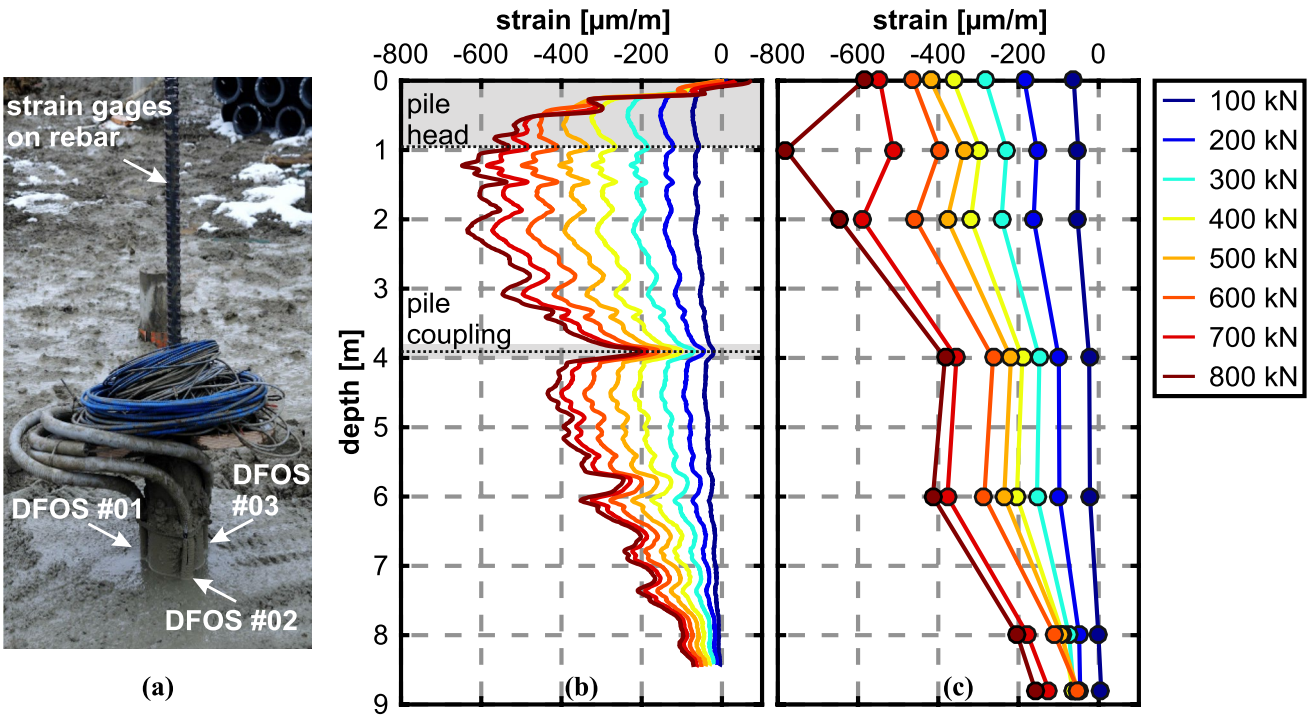

Fig. 7 Comparison between internal electrical and fiber optic strain measurements along the pile [17]: **a** positions of sensors; **b** mean strain profiles derived from DFOS sensing cables; **c** strain profiles measured by strain gages along the installed rebar

$$\kappa_i = \frac{\epsilon_{i,3} - \epsilon_{i,1}}{h\,(1 + \epsilon_i)}, \tag{2}$$

where h is the known distance between the optical fiber cores and ϵ_i is the mean strain at the considered depth (already shown in Fig. 7b).

The measured strain profiles during the compression test along the optical sensing cables DFOS #01 and #03 in the upper section of the pile are displayed in Fig. 8 (a), (b). These depict significant deviations in the strain distribution in the area between 0.0 and 3.0 m, from which the curvature distribution along the pile can be derived with the known distance between the fibers of about 125 mm. The determined curvature profiles in Fig. 8 (c) show that bending along the pile and the grout material becomes visible during pile testing, which suggests that the ductile pile was not driven completely vertical into the soil. Consequently, the surrounding grout material took a curved shape and varying cross-sectional profile of the grout arose along the pile. It has to be noted that a curved shape already existed after construction of the pile before the DFOS zero measurement was taken. All displayed DFOS results are relative to the zero measurement made just before the beginning of the load test. From the measurement results, it can be concluded that the curvature of the pile increased even further when the load test was performed. The total curvature amount in transversal direction can, however, not be derived from the conducted measurements.

The upper section of the pile of about 2.5 m was excavated after the test (Fig. 8d). The captured situation depicts the curved shape of the grout material and verifies the assumption concluded above. The "screwed pile" is a result of a special conical driving shoe that was tested during the construction of this pile and does not appear in the conventional driving setup. The DFOS system is, however, able to monitor the curvature effects and finally allows a detailed study of the pile driving process.

Especially in applications with critical buried infrastructure (e.g. pipelines), the curvature of an object represents a critical parameter in the context of structural health monitoring. DFOS systems enable the distributed curvature assessment over long distances and allow the localization of critical events along the object, see, e.g. [5, 11].

5 Continuous monitoring

The designed DFOS approach was also utilized for a continuous monitoring of ductile driven piles, which were used for the foundation of a construction pit. The construction

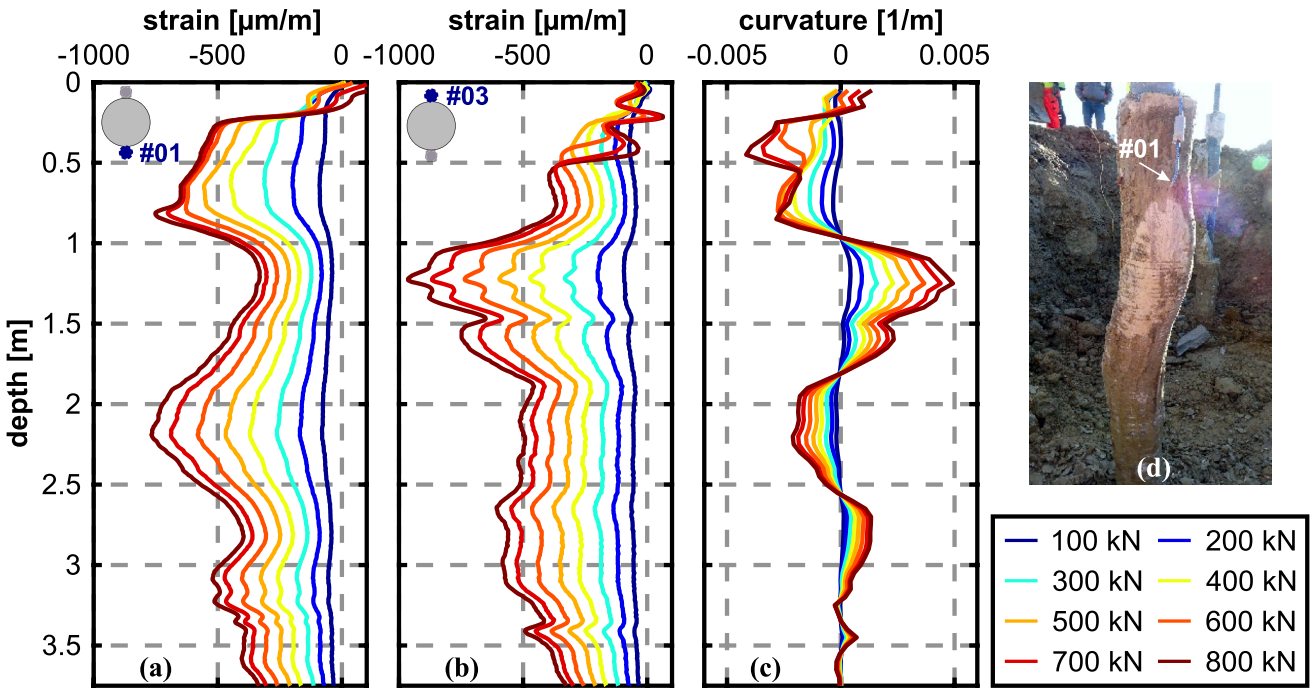

Fig. 8 Evaluation of curvature effects along the installed ductile pile [21]: **a** strain profiles along DFOS #01; **b** strain profiles along DFOS #03; **c** derived curvature response; **d** excavation of the piles' upper part

site itself is characterized by special soil and groundwater conditions: the first 5 to 8 m consists of floodplain sediments followed by massive basin sediments down to a depth of about 20 to 25 m. Beneath, a moraine provides a capable, load-bearing layer for the pile foundation. The supporting of the construction pit's excavation was performed by sheet pile walls. These, however, could not be anchored due to neighboring constructions why a reinforced base plate was used to brace the pit. The construction of the first piles showed that substantial efforts were required to pump the grout material into the ground and uplifts of the base plate as well as of the sheet pile walls in the range of centimeters could be recognized. It was assumed that the high-density soil with constant volume displaces the installed piles after the installation, which causes an uplift of the pile and obviously also an uplift of the entire construction pit.

To analyze the monitored behavior in more detail, the DFOS system should clarify if either the piles failed and were pulled apart at one of the conical collars or the whole piles were pushed out of the ground. The distributed strain profiles should also provide information about the load transfer from the soil to the pile. Therefore, the DFOS system was installed along three selected piles with lengths of up to 25 m. Beside the strain sensing cable V3, an additional temperature sensing cable [29] was installed along each pile, which can be used for temperature compensation. In total, seven individual cables were guided from the pile head to a temperature-regulated container. Autonomous monitoring was performed over almost three weeks with a temporal resolution of 1 h using the OBR 4600 in combination with an optical switch to enable autonomous sequential measurements of the installed sensing cables.

The measured DFOS strain profiles of one selected pile on each day over the entire monitoring period are depicted in Fig. 9. During the first days until 08/05, a continuous increase of compression strain is visible along the entire pile with slight variations at the pile head and at depths higher than 20 m. Immediately after the installation of the next piles starting from 08/05, tensile stresses arise in the bottom area, which segue into compressional stresses with decreasing depth. No conspicuous behavior can be observed at the pile couplings. This suggests that the entire pile is pushed out of the ground from beneath and compressed at the pile head due to interaction with the base plate. In the following, slight releases of the tensile stresses can be observed starting from 08/09.

It is obvious that the working progress on-site has major influence on the pile behavior. For detailed analysis, Fig. 10 displays the displacements determined from the DFOS strain profiles at the pile head over the entire monitoring period and the minimum working distance to the instrumented DFOS pile per day. Thereby, the derived deformation can be exactly related to the current working steps: decreasing strain over time is visible on weekends (gray areas in Fig. 10), where no work was carried out. If piles were constructed nearby the DFOS pile (distance $< 3\ m$, red areas in

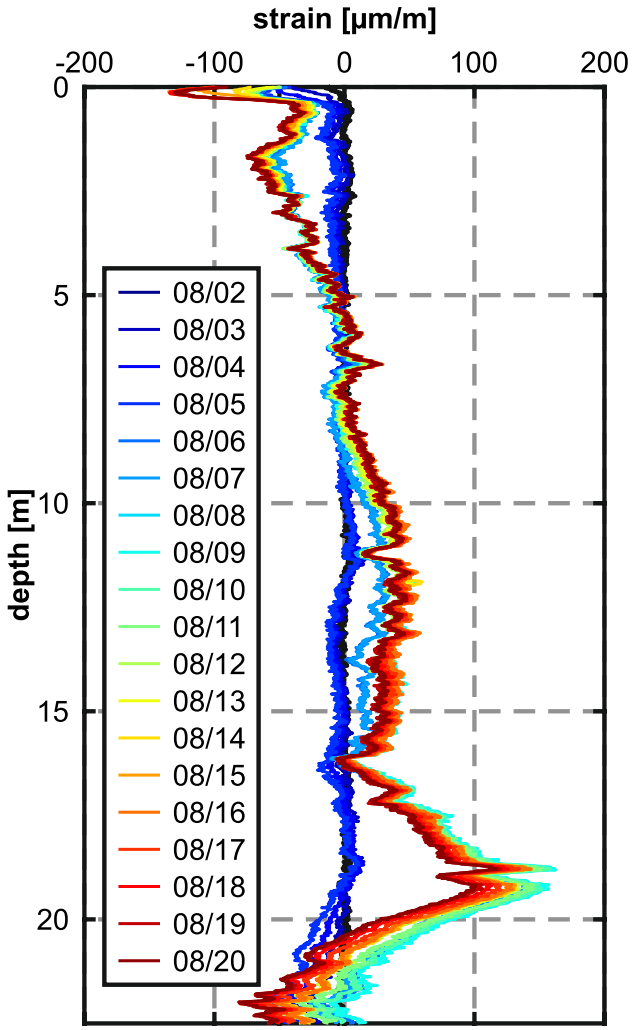

Fig. 9 Strain profiles along the instrumented DFOS pile measured at each day of the continuous monitoring from 2nd to 20th of August 2019

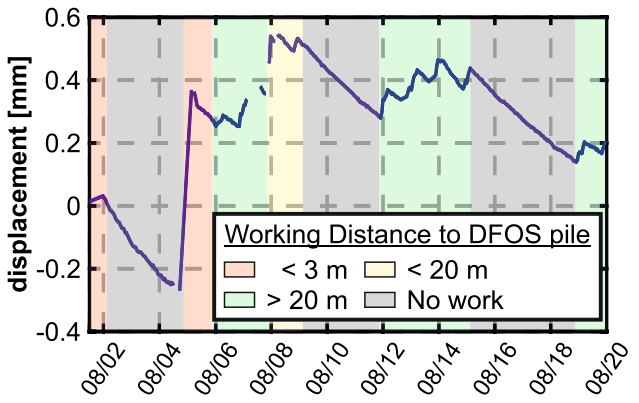

Fig. 10 Displacements derived from DFOS strain profiles at the pile head over entire continuous monitoring campaign

Fig. 10), the displacement increase can be observed instantly (e.g. 08/05) compared to times, when the construction was performed farther away (distance $> 20\,m$, green areas in Fig. 10, e.g. 06 to 08/08), which also confirms the above-drawn assumption regarding the pile uplift as a result of the high-density soil.

6 Conclusion

In this paper, we have shown a sensing approach based on DFOS, which enables distributed strain measurements along driven ductile piles. To ensure the integrity of the optical fiber during the pile construction and monitoring in harsh field environment, robust sensing cables and reliable installation techniques were found. The results of various field applications demonstrate the high potential of the DFOS system, which delivers information that cannot be measured using other techniques, especially due to the high spatial resolution of about 10 mm.

Load tests in different soils have shown that the prevalent soil conditions can be related to the measured strain distributions, which are basically also confirmed by results of dynamic probing nearby the installed piles. Nevertheless, detailed investigations on the material properties, i.e. wall thickness measurements and detailed recording of the grouting diameter, will be carried out at future construction sites to enable further analysis on the correlations. The results of the DFOS system agree with measurements of electrical distance transducers at the pile head as well as internal pointwise strain gauges along an additionally installed reinforcement bar. Due to the arrangement of the optical fibers, curvature changes in transversal direction of the pile can also be identified.

Autonomous measurements of pile uplifts on-site over almost 3 weeks demonstrate the suitability of the designed DFOS approach for field applications. The measured strain profiles can be clearly related to the working progress and confirm that the observed uplifts were mostly caused by absolute movements of the pile and not by failures at the pile couplings.

The DFOS approach can also be used to detect arising cracks in the grout material due to its progressive failure. As a result of the protection layers of the sensing cables, the measured profiles depict an integrative, smoothed strain response depending on the used cable type. Future research will be especially focused on the interaction of the different sensing cables and the surrounding grout material. This, however, requires a detailed modeling of the sensing cable design (see [3, 9]) as well as detailed laboratory investigations, which shall prove the modeling suitability to determine the effective crack widths inside the grout.

Acknowledgements Open access funding provided by Graz University of Technology. The authors would like to thank all project partners, especially Keller Grundbau Ges.mbH for the opportunity to realize various field applications using the developed DFOS system, the IGMS team members (Dietmar Denkmaier, Ferdinand Klug, Madeleine Winkler, Helmut Woschitz) for their valuable efforts during the installations and the University of Kassel (Department of Geotechnology and Geohydraulics) for providing the data of the internal strain gauge measurements.

Compliance with ethical standards

Conflict of interest The authors declare that they have no conflict of interest.

Disclaimer This article is an extended version of the conference paper "5 years" experience using distributed fiber optic sensing along ductile driven piles" presented at the 9th International Conference on Structural Health Monitoring of Intelligent Infrastructure, which was held in St. Louis, Missouri from 4th to 7th of August 2019.

References

1. Bersan S, Bergamo O, Palmieri L, Schenato L, Simonini P (2018) Distributed strain measurements in a cfa pile using high spatial resolution fibre optic sensors. Eng Struc 160:554–565. https://doi.org/10.1016/j.engstruct.2018.01.046
2. Feng X, Han Y, Wang Z, Liu H (2018) Structural performance monitoring of buried pipelines using distributed fiber optic sensors. J Civil Struc Health Monitor 8(3):509–516. https://doi.org/10.1007/s13349-018-0286-3
3. Feng X, Zhou J, Sun C, Zhang X, Ansari F (2013) Theoretical and experimental investigations into crack detection with botdr-distributed fiber optic sensors. Eng Mechan 139(12):1797–1807. https://doi.org/10.1061/(ASCE)EM.1943-7889.0000622
4. Forbes B, Vlachopoulos N, Hyett A, Diederichs M (2017) A new optical sensing technique for monitoring shear of rock bolts. Tunnell Underground Space Technol 66:34–46. https://doi.org/10.1016/j.tust.2017.03.007
5. Glisic B, Yao Y (2012) Fiber optic method for health assessment of pipelines subjected to earthquake-induced ground movement. Struct Health Monitor 11(6):696–711. https://doi.org/10.1177/1475921712455683
6. Glišić B, Inaudi D (2007) Fibre optic methods for structural health monitoring. John Wiley & Sons Ltd., US
7. Hartog A (2017) An introduction to distributed optical fibre sensors. CRC Press, Taylor & Francis Group. https://doi.org/10.1201/9781315119014
8. Hayden M, Kirchmaier T (2010) Pile HAY-Proof-System ® (Pile H-P-S) – Neuartiges System für statische Probebelastungen an schlanken Pfählen. In: Proc. 25th Christian Veder Colloquium. Graz University of Technology
9. Henault JM, Salin J, Moreau G, Quiertant M, Taillade F, Benzarti K, Delepine-Lesoille S (2012) Analysis of the strain transfer mechanism between a truly distributed optical fiber sensor and the surrounding medium. In: Proc. 3rd International Conference on Concrete Repair, Rehabilitation and Retrofitting (ICCRRR 2012). pp. 1002–1013
10. Hong CY, Zhang YF, Liu L (2016) Application of distributed optical fiber sensor for monitoring the mechanical performance of a driven pile. Measurement 88:186–193. https://doi.org/10.1016/j.measurement.2016.03.052
11. Inaudi D, Glišić B (2010) Long-range pipeline monitoring by distributed fiber optic sensing. Pressure Vessel Technol 132:011701–9. https://doi.org/10.1115/1.3062942
12. Klais F, Wolf P, Lienhart W (2017) The grautschenhof contract - construction of an intermediate access under complex local conditions. Geomechan Tunnell 10(6):686–693. https://doi.org/10.1002/geot.201700052
13. Li Z (2018) Distributed fibre optic sensing of a deep excavation adjacent to pre-existing tunnels. Géotechnique Lett. https://doi.org/10.1680/jgele.18.00031
14. Lienhart W, Buchmayer F, Klug F, Monsberger CM (2019) Distributed fiber optic sensing on a large tunnel construction site: Increased safety, more efficient construction and basis for condition–based maintenance. In: International Conference on Smart Infrastructure and Construction 2019 (ICSIC). pp. 595–604 https://doi.org/10.1680/icsic.64669.595
15. López-Higuera JM (2002) Handbook of Optic Fibre Sensing Technology. John Wiley & Sons Ltd, US
16. Luna Technologies Inc. (2019) OBR 4600 Optical Backscatter Reflectometer, Datasheet. Roanoke, VA, USA. https://lunainc.com/wp-content/uploads/2012/11/LUNA-Data-Sheet-OBR-4600-V2.pdf (Accessed: Apr. 04, 2019)
17. Monsberger C, Winkler M, Woschitz H, Lienhart W, Hayden M (2019) 5 years' experience using distributed fiber optic sensing along ductile driven piles. In: 9th International Conference on Structural Health Monitoring of Intelligent Infrastructure (SHMII-9). International Society for Structural Health Monitoring of Intelligent Infrastructure
18. Monsberger C, Woschitz H, Hayden M (2016) Deformation measurement of a driven pile using distributed fibre-optic sensing. J Appl Geodesy 10(1):61–69. https://doi.org/10.1515/jag-2015-0021
19. Monsberger C, Woschitz H, Lienhart W, Račanský V, Hayden M (2017) Performance assessment of geotechnical structural elements using distributed fiber optic sensing. In: Proc. SPIE 10168, Sensors and Smart Structures Technologies for Civil, Mechanical, and Aerospace Systems, pp. 101680Z, 1–12. International Society for Optics and Photonics
20. Monsberger CM, Lienhart W (2019) Design, testing, and realization of a distributed fiber optic monitoring system to assess bending characteristics along grouted anchors. J Lightwave Technol 37(16):4603–4609. https://doi.org/10.1109/JLT.2019.2913907
21. Monsberger CM, Lienhart W (2019) In-situ assessment of curvature and bending characteristics along geotechnical structures using distributed fiber optic sensors. In: Proceedings of the 12th International Workshop on Structural Health Monitoring 2019: Enabling Intelligent Life-cycle Health Management for Industry Internet of Things (IIOT). pp. 1715–1723. DEStech Publications, Inc
22. Moser F, Lienhart W, Woschitz H, Schuller H (2016) Longterm monitoring of reinforced earth structures using distributed fiber optic sensing. J Civil Struct Health Monitor 6(3):321–327

23. OZ Optics Ltd. (2018) Fiber Optic Distributed Strain and Temperature Sensors (DSTS) BOTDA Module. Ottawa, Canada. https://www.ozoptics.com/ALLNEW_PDF/DTS0115.pdf (Accessed: May 26, 2019)
24. Pelecanos L, Soga K, Elshafie MZEB, de Battista N, Kechavarzi C, Gue CY, Ouyang Y, Seo HJ (2018) Distributed fiber optic sensing of axially loaded bored piles. J Geotechn Geoenvironm Eng 144(3):1–16. https://doi.org/10.1061/(ASCE)GT.1943-5606.0001843
25. Pelecanos L, Soga K, Hardy S, Blair A, Patel D (2016) Distributed fibre optic monitoring of tension piles under a basement excavation at the v&a museum in london. In: Proceedings of the International Conference on Smart Infrastructure and Construction 2016 (ISIC). https://doi.org/10.1680/tfitsi.61279.057
26. Rui Y, Kechavarzi C, O'Leary F, Barker C, Nicholson D, Soga K (2017) Integrity testing of pile cover using distributed fibre optic sensing. Sensors 17(12), https://doi.org/10.3390/s17122949
27. Solifos AG (2019) BRUsens DSS 3.2mm V9 grip 3_50_2_005. Windisch, Switzerland (Oct. 31). http://solifos.nubosys.com/fileadmin/syncfiles/media/Solifos_SE-01-03_3-50-2-005_en.pdf (Accessed: Jan. 22, 2020)
28. Solifos AG (2019) BRUsens DSS 7.2mm V3 grip 3_50_2_002. Windisch, Switzerland (Oct. 31). http://solifos.nubosys.com/fileadmin/syncfiles/media/Solifos_SE-01-03_3-50-2-002_en.pdf (Accessed: Jan. 22, 2020)
29. Solifos AG (2019) BRUsens DTS STL PA 3_50_1_001. Windisch, Switzerland (Oct. 31). http://solifos.nubosys.com/fileadmin/syncfiles/media/Solifos_SE-01-01_3-50-1-001_en.pdf (Accessed: Jan. 22, 2020)
30. Wagner L, Kluckner A, Monsberger CM, Wolf P, Prall K, Schubert W, Lienhart W (2020) Direct and distributed strain measurements inside a shotcrete lining: Concept and realisation. Rock Mechan Rock Eng 53:641–652. https://doi.org/10.1007/s00603-019-01923-4
31. Woschitz H, Klug F, Lienhart W (2015) Design and calibration of a fiber-optic monitoring system for the determination of segment joint movements inside a hydro power dam. J Lightwave Technol 33(12):2652–2657